Received: 15 January 2020 | Revised: 18 May 2020 | Accepted: 31 May 2020

DOI: 10.1002/nme.6451

RESEARCH ARTICLE

WILEY

Multifidelity adaptive kriging metamodel based on discretization error bounds

L. Mell | **V. Rey** | **F. Schoefs**

GeM-Institut de Recherche en Génie Civil et Mécanique-UMR 6183-CNRS-Université de Nantes, Ecole Centrale de Nantes Nantes- 2, Nantes, France

Correspondence
V. Rey, GeM-Institut de Recherche en Génie Civil et Mécanique-UMR 6183-CNRS- Université de Nantes, Ecole Centrale de Nantes Nantes- 2, rue de la Houssinière - BP 92208 44322 Nantes CEDEX 3, France.
Email: valentine.rey@univ-nantes.fr

Funding information
Conseil Régional des Pays de la Loire

Summary

This article presents an approach to build a multifidelity kriging metamodel from finite element computations on different meshes for stuctural reliability assessment. The proposed method takes advantage of the computation of bounds on the discretization error, which enables to guarantee the state (safe or failure) of each computation of the performance function. An algorithm to build the metamodel from the different levels of fidelity and estimate the failure probability is provided. Illustrations are presented on a two dimensional mechanical crack opening problem. Bounds on the failure probability are also post-processed.

KEYWORDS

error estimation, finite element method, kriging methods, probability of failure, reliability analysis

1 | INTRODUCTION

Uncertainties may arise from a lack of knowledge (for example, characterization of material properties can be improved) or from inherent variability (an example is the load due to wind flow on the blade of a wind turbine).

As a consequence, designing structures subjected to uncertainty in a deterministic framework becomes impractical. As aftermaths in case of failure are sometimes dramatic, the reliability analysis becomes crucial and sensitive. This safety analysis is usually done in a probabilistic approach that aims at estimating quantities such as the probability of failure, reliability indexes, sensitivity factors, and so on.

In the context of virtual testing for numerical certification of structures, the probability of failure is usually computed using numerical simulations of a model of the structure. Different strategies can be considered. First, sampling techniques that mainly rely on Monte Carlo or quasi Monte Carlo simulations[1] present the advantage of being nonintrusive. Besides, their efficiency does not depend on the number of random variables, making them attractive. Their main disadvantage is that the convergence rate against the number of samples is very low, so that they are computationally expensive. To tackle this issue, reduction of variance or multilevel Monte Carlo approach have been proposed.[2,3] Second, approximation methods aim at searching for a random field in a given approximation space, the Galerkin method[4] is an example of them. When the geometry of the structure is random, methods such as XSFEM have been developed.[5,6] However, those techniques can be intrusive.

The reduction of computational costs can also be done using surrogate models. First, polynomial response surfaces were developed.[7] Then, kriging-based metamodels[8,9] became very popular in the field of safety analysis. The most popular method was developed in.[10] It was then adapted to very low probability using important sampling or subset sampling[11,12] and finally to system reliability.[13] The main asset of kriging is that it offers an indicator of the quality of the metamodel.

Indeed this method considers that the metamodel is a realization of a random Gaussian process, the standard deviation of this process is then computable at each point where the metamodel is evaluated.

Two components of the mechano-probabilistic problem may affect the accuracy of the reliability assessment: epistemic uncertainties on some parameters (including model parameters) and the inaccuracy of the numerical solution to the mechanical problem. To deal with epistemic uncertainties on parameter, References 14 and 15 propose a projection method to propagate through the mechanical model bounds on these variable to obtain bounds on the probability of failure. Few people consider the error due to the discretization method (mainly the finite element method). Yet, this error may lead to a poor estimation of the probability of failure, as illustrated in Reference 16. Performing numerical simulations on too coarse meshes might in fact lead to considering that a realization belongs to the safety domain while it actually belongs to the failure domain. Among works tackling this issue, Reference 17 can be cited. It uses the discretization error introduced by meshing using the Richardson extrapolation in a nondeterministic analysis. In Reference 18, the Richardson extrapolation is also used to perform reliability analysis with the first-order reliability method (FORM).[19] In Reference 20, the author estimates the probability of failure using FORM while utilizing the discretization error to provide bounds on the probability of failure.

In the family of kriging techniques, multifidelity kriging consists in using several models with different precision to build a multifidelity metamodel. The main objective of this approach is to obtain an improved trade-off between computational cost and precision by choosing to evaluate some samples on a low fidelity model and some others on a high fidelity one. In Reference 21, optimization in the context of a fluid flow problem is performed with progressively fine grids. In References 22 and 23, multifidelity kriging is performed on a flow problems. In the context of optimization, References 24 and 25 adapt the stopping criterion of the iterative contact solver to use multifidelity kriging. In Reference 26, a multifidelity approach is used on a elasto-viscoplasticity problem with different proper generalized decompositions. It is to be noted that usually, the choice of levels of discretization or grids is done a priori and the construction of the design of experiments is based on heuristics.

In this article, we propose an adaptive multifidelity kriging approach to estimate the probability of failure. This method uses the estimation of the discretization error to choose a suitable mesh for each sampling point by noting that only the sign of the limit state function is of importance: the reliability problem is considered as a classification problem. In addition to the estimation of the probability of failure, the method gives lower and upper bounds on the exact probability of failure.

The article is organized as follow. In Section 2, we define the mechanical problem and recall the kriging-based meta model approach used to estimate the failure probability. In Section 3, we present the approach we propose to build a multifidelity kriging metamodel and its application to compute the probability of failure. In Section 4, we apply our method to a crack-opening problem. Finally, Section 5 concludes the article.

2 | SETTINGS

In this section, the continuous mechanical problem and its discretized version are first defined. Then, the discretization error and its estimates are presented. Finally, we define the limit-state functions and formulate the reliability assessment in terms of estimation of the probability of failure.

2.1 | Continuous problem

Let $\mathbb{R}^d$ represent the physical space. Let us consider the static equilibrium of a (polyhedral) structure occupying the open domain $\Omega \subset \mathbb{R}^d$ and subjected to a given body force f within Ω, to a given traction force $\underline{F}$ on $\partial_F\Omega$ and to a given displacement field u_d on the complementary part $\partial_u\Omega \neq \emptyset$. Let us assume the structure undergoes small perturbations and that the material is linear elastic, characterized by Hooke's elasticity tensor H. Let u be the unknown displacement field, $\varepsilon(u)$ the symmetric part of the gradient of $\underline{u}$, and $\underline{\underline{\sigma}}$ the Cauchy stress tensor.

Two affine subspaces and a positive form are introduced:

- The affine subspace of kinematically admissible fields (KA-fields)

$$\mathrm{KA} = \{\underline{u} \in (\mathrm{H}^1(\Omega))^d,\ \underline{u} = \underline{u}_d \ \text{ on } \ \partial_u\Omega\}, \tag{1}$$

and we note KA^0 the associated vectorial space.

- Affine subspace of statically admissible fields (SA-fields)

$$\begin{aligned} SA = \{&\underline{\underline{\tau}} \in (L^2(\Omega))^{d\times d}_{sym}; \forall \underline{v} \in KA^0, \\ &\Omega \int \underline{\underline{\tau}} : \underline{\underline{\varepsilon}}(\underline{v})\, d\Omega = \omega \int \underline{f} \cdot \underline{v} d\Omega + \partial_F \Omega \int \underline{F} \cdot \underline{v} dS\}. \end{aligned} \tag{2}$$

- Error in constitutive equation

$$e_{CR_\Omega}(\underline{u}, \underline{\underline{\sigma}}) = \|\underline{\underline{\sigma}} - \mathbb{H} : \underline{\underline{\varepsilon}}(\underline{u})\|_{\mathbb{H}^{-1},\Omega}, \tag{3}$$

where $\|\underline{\underline{x}}\|_{\mathbb{H}^{-1},\Omega} = \sqrt{\int_\Omega (\underline{\underline{x}} : \mathbb{H}^{-1} : \underline{\underline{x}}) d\Omega}$.

The continuous problems reads:

$$\begin{cases} \text{Find a displacement field } \underline{u} \text{ and a stress field } \underline{\underline{\sigma}} \text{ such that} \\ \underline{u} = \underline{u}_d \text{ on } \partial\Omega \cap \partial_u\Omega \text{ and } \underline{\underline{\varepsilon}}(\underline{u}) = \frac{1}{2}(\underline{\underline{grad}}(\underline{u}) + \underline{\underline{grad}}^T(\underline{u})) \text{ on } \Omega \\ \underline{\mathrm{div}}(\underline{\underline{\sigma}}) + \underline{f} = \underline{0} \text{ on } \Omega \text{ and } \underline{\underline{\sigma}}\underline{n} = \underline{F} \text{ on } \partial_F\Omega \\ \underline{\underline{\sigma}} = \mathbb{H} : \underline{\underline{\varepsilon}}(\underline{u}) \text{ on } \Omega \end{cases} \tag{4}$$

The solution to this problem exists and is unique. We will denote the couple displacement field and stress field as the exact solution.

The mechanical problem can also be formulated as:

Find $(\underline{u}_{ex}, \underline{\underline{\sigma}}_{ex}) \in KA \times SA$ such that $e_{CR\Omega}(\underline{u}_{ex}, \underline{\underline{\sigma}}_{ex}) = 0$.

2.2 | Discrete problem

Let Ω_H be a tessellation of $\overline{\Omega}$ by triangles. The finite element method consists in searching for a displacement field in the finite subspace KA_H of KA where KA_H reads:

$$KA_H = \{\underline{u} \in (H^1(\Omega))^d,\ \underline{u} = \underline{u}_d \text{ on } \partial_u\Omega_H\}. \tag{5}$$

The discrete problem can be formulated as:

$$\begin{aligned} &\underline{u}_H \in KA_H \\ &\underline{\underline{\sigma}}_H = \mathbb{H} : \underline{\underline{\varepsilon}}(\underline{u}_H) \\ &\int_{\Omega_H} \underline{\underline{\sigma}}_H : \underline{\underline{\varepsilon}}(\underline{v}_H) d\Omega = \int_{\Omega_H} \underline{f} \cdot \underline{v}_H d\Omega + \int_{\partial_F\Omega_H} \underline{F} \cdot \underline{v}_H dS \cdot \forall \underline{v}_H \in KA^0_H \end{aligned} \tag{6}$$

The solution of this discrete problem exists and is unique. However, the discrete solution $\underline{u}_H$ usually does not coincide with the continuous exact solution $\underline{u}_{ex}$.

2.3 | Estimation of the discretization error

2.3.1 | Generalities

Since the discrete displacement field $\underline{u}_H$ is not the exact solution, the finite element method introduces an error usually called discretization error. Results on the convergence of the FEM offer an a priori estimate of this error. It involves

problem dependent constants that are not computable thus making this error estimate impractical. One can also use a posteriori error estimator that rely on a post-process of the finite element solution to derive an estimation of the discretization error.[27] In this article, estimators based on the error in constitutive relation (3) were chosen as they provide guaranteed error bounds.[28] These estimators are based on the fundamental relation:

$$\forall(\underline{\hat{u}}, \underline{\underline{\hat{\sigma}}}) \in \mathrm{KA}(\Omega) \times \mathrm{SA}(\Omega),$$

$$\|\underline{\underline{\varepsilon}}(\underline{u}_{ex}) - \underline{\underline{\varepsilon}}(\underline{\hat{u}})\|^2_{\mathbb{H},\Omega} + \|\underline{\underline{\sigma}}_{ex} - \underline{\underline{\hat{\sigma}}}\|^2_{\mathbb{H}^{-1},\Omega} = e^2_{CR_\Omega}(\underline{\hat{u}}, \underline{\underline{\hat{\sigma}}}). \tag{7}$$

We note $|||\underline{v}|||_\Omega = \|\underline{\underline{\varepsilon}}(\underline{v})\|_{\mathbb{H},\Omega}$ the energy norm of the displacement. By choosing $\underline{\hat{u}} = \underline{u}_H \in \mathrm{KA}(\Omega)$, we obtain the following upper bound for the error $\underline{e}_{discr} = \underline{u}_{ex} - \underline{u}_H$:

$$e_{discr} := |||e_{discr}|||_\Omega \leqslant e_{CR_\Omega}(\underline{u}_H, \underline{\underline{\hat{\sigma}}}). \tag{8}$$

Computing a statically admissible stress field is a complex task but several methods have been developed to compute $\underline{\underline{\hat{\sigma}}} \in \mathrm{SA}(\Omega)$ (see References 29-32).

However, this global energetic information on the discretization error may be useless for practical application. Therefore, goal-oriented error aims at providing bounds on the error on a quantity of interest. In this article, the quantity of interest is considered to be a linear form of the displacement field, defined by extractors.[33]

2.3.2 | Definition of the linear quantity of interest and the adjoint problem

In reliability, the quantity of interest is defined as a function of performance defining the domain of failure and of safety. This performance function is also called limit state function and is written as a margin between a resistance R and a solicitation S. The resistance is either deterministic or random. This limit state function may be written :

$$g = R - S. \tag{9}$$

The sign of this function defines the failure or not of the structure. To estimate bounds on the quantity g, the solicitation S needs to be defined by a linear functional $\tilde{L}$:

$$g = R - \tilde{L}(\underline{u}) = R - \int_\Omega (\underline{\underline{\sigma}}_\Sigma : \underline{\underline{\varepsilon}}(\underline{u}) + \underline{f}_\Sigma \underline{u}) d\Omega, \tag{10}$$

where $\underline{\underline{\sigma}}_\Sigma$ and $\underline{f}_\Sigma$ are extractors. It is possible to treat non linear quantities of interest. For some of them, there are specific methods to calculate guaranteed bounds.[34,35] Otherwise, this quantity would need to be linearized. It would result in the loss of the guarantee that g_{ex} lies between estimated bounds. Finally, the probability of failure that will later be estimated is likely to be biased. We define the subspace of statically admissible fields for the adjoint problem:

$$\tilde{\mathrm{SA}}(\omega) = \{\underline{\underline{\tau}} \in (\mathrm{L}^2(\omega))^{d\times d}_{\mathrm{sym}};\ \forall \underline{v} \in \mathrm{KA}^{00}(\omega),\ \omega \int \underline{\underline{\tau}} : \underline{\underline{\varepsilon}}(\underline{v}) d\omega = \tilde{L}(\underline{v})\}. \tag{11}$$

The adjoint problem set on Ω reads:

$$\text{Find } (\underline{\tilde{u}}_{ex}, \underline{\underline{\tilde{\sigma}}}_{ex}) \in \mathrm{KA}^0(\Omega) \times \tilde{\mathrm{SA}}(\Omega) \text{ such that } e_{CR_\Omega}(\underline{\tilde{u}}_{ex}, \underline{\underline{\tilde{\sigma}}}_{ex}) = 0. \tag{12}$$

The solution to this problem exists and is unique.

The adjoint problem is usually solved using the finite element method. The mesh does not need to be the same as for the forward problem. The adjoint displacement field obtained by solving the adjoint problem with the FEM is $\underline{\tilde{u}}_{\tilde{H}}$.

We define the discretization error of the adjoint problem as:

$$e_{discr} = |||\tilde{e}_{discr}|||_{\Omega} = |||\underline{\tilde{u}}_{ex} - \underline{\tilde{u}}_{\tilde{H}}|||_{\Omega}. \tag{13}$$

2.3.3 | Error estimation on a quantity of interest

We denote $g_{ex} = R - \tilde{L}(\underline{u}_{ex})$ the unknown exact value of the limit state function. $g_H = R - \tilde{L}(\underline{u}_H)$ is an approximation of this quantity of interest.

Bounds from References 36 and 37 can be applied to the quantity of interest g_{ex}:

$$|g_{ex} - g_H + I_{HH}| \leq \frac{1}{2} e_{CR_{\Omega}}(\underline{u}_H, \underline{\underline{\hat{\sigma}}}_H) e_{CR_{\Omega}}(\underline{\tilde{u}}_{\tilde{H}}, \underline{\underline{\hat{\tilde{\sigma}}}}_{\tilde{H}}), \tag{14}$$

where

$$I_{HH} = \Omega \int \frac{1}{2} (\underline{\underline{\hat{\tilde{\sigma}}}}_{\tilde{H}} + \mathbb{H} : \underline{\underline{\varepsilon}}(\underline{\tilde{u}}_{\tilde{H}})) : \mathbb{H}^{-1} : (\underline{\underline{\hat{\sigma}}}_H - \mathbb{H} : \underline{\underline{\varepsilon}}(\underline{u}_H)) d\Omega, \tag{15}$$

and where $\underline{\underline{\hat{\tilde{\sigma}}}}_{\tilde{H}} \in \tilde{SA}_H(\Omega)$.

Therefore, the error on the quantity of interest can be obtained from the product of the two errors in energy norm of both reference and adjoint problem. In this article, we choose to solve both reference and adjoint problems on the same mesh so that it does not require an additional factorization of the stiffness matrix. Solving the finite element problem is in fact simplified to a multiple (double) right-hand side linear equation.

It is to be noted that the bounds provided here do not guarantee that g_H is inside them. In fact, for the structure studied in Section 4, the finite element solution is outside the bounds. It would be absurd to use a value that is guaranteed to be false. Therefore, it was decided to use the middle of the bounds as the output of the finite element code:

$$g^m = g_H - I_{HH}. \tag{16}$$

In fact, it was observed in Reference 38 that g^m is in most cases a better approximation of the true value g_{ex}. A bounding of g_{ex} is, therefore:

$$g^- \leq g_{ex} \leq g^+, \tag{17}$$

where

$$g^- := g^m - \frac{1}{2} e_{CR_{\Omega}}(\underline{u}_H, \underline{\underline{\hat{\sigma}}}_H) e_{CR_{\Omega}}(\underline{\tilde{u}}_{\tilde{H}}, \underline{\underline{\hat{\tilde{\sigma}}}}_{\tilde{H}}), \tag{18}$$

and

$$g^+ := g^m + \frac{1}{2} e_{CR_{\Omega}}(\underline{u}_H, \underline{\underline{\hat{\sigma}}}_H) e_{CR_{\Omega}}(\underline{\tilde{u}}_{\tilde{H}}, \underline{\underline{\hat{\tilde{\sigma}}}}_{\tilde{H}}). \tag{19}$$

2.4 | Estimation of the probability of failure

For the sake of simplicity, in the previous subsection, the mechanical problem is presented as deterministic. In reality, the geometry, the loading, or the behavior of the structure is random and as a consequence, the displacement fields $\underline{u}_{ex}$ and u_H are random fields.

We gather the n random variables of the mechanical problem into a random vector $\{X\}$ with joint probability density $f_{\{X\}}(\{x\})$.

The exact probability of failure $P_{f,ex}$ is defined from the exact displacement solution $\underline{u}_{ex}$ via the exact limit state function g_{ex}:

$$P_{f,ex} = \int_{g_{ex}(\{X\})\leq 0} f_{\{X\}}(\{x\})dx_1 \ \dots \ dx_n. \tag{20}$$

The probability of failure computed using the finite element solution u_H is found by replacing the limit state function g_{ex} by g_H. As a consequence, the discretization error leads to an error on the estimation of the probability of failure since $P_{f,H} \neq P_{f,ex}$.

In addition, the form of the limit-state function is usually unknown and surrogates techniques aim at building an approximation $\hat{g}$ of g using samples. In this article, we will consider that $\hat{g}$ is built using kriging techniques. One can define the probability of failure computed using the surrogate model $\hat{g}$ built from the exact mechanical solutions:

$$\hat{P}_{f,ex} = \int_{\hat{g}_{ex}(\{X\})\leq 0} f_{\{X\}}(\{x\})dx_1 \ \dots \ dx_n. \tag{21}$$

Therefore, the metamodeling error leads to an error in the estimation of the probability of failure as $\hat{P}_{f,ex} \neq P_{f,ex}$.

Since the exact solution is almost never known, the samples used to construct the surrogate model are computed with finite element solutions so that the probability of failure is

$$\hat{P}_{f,H} = \int_{\hat{g}_H(\{X\})\leq 0} f_{\{X\}}(\{x\})dx_1 \ \dots \ dx_n. \tag{22}$$

The only difference between integrals (20), (21), and (22) is the domain of integration that is defined by the limit state $g = 0$. Therefore, the assessment of the probability of failure can be seen as a classification problem for which only the limit state needs to be precisely characterized.

3 | MULTIFIDELITY KRIGING FOR RELIABILITY ANALYSIS

In this section, we first explain the principle of kriging and its application to the estimation of failure probabilities $\hat{P}_{f,ex}$ and $\hat{P}_{f,H}$. Then, we propose a methodology to construct a kriging-based multifidelity surrogate model exploiting the discretization error bounds. The objective will be to classify evaluations of g correctly ($g \leq 0$ means the sample is failed and $g > 0$ means safe).

3.1 | Kriging

Metamodeling consists in computing an estimation of a quantity of interest cheaper to evaluate than the initial function g, where g can either be g_{ex} or g_H.

Let consider that m observations (or computations) at $\underline{x}_1^{obs} \ \dots \ \underline{x}_m^{obs}$ of g are gathered in a vector of observations $\underline{g}^{obs}$.

Kriging[8] relies on the hypothesis that the objective function g is the realization of a stationary Gaussian process G

$$G(\underline{x}) = y(\underline{x}) + Z(\underline{x}), \tag{23}$$

where $\underline{x} \in \mathbb{R}^n$, $y(\underline{x})$ is the mean of $G(\underline{x})$ and $Z(\underline{x})$ is a random variable distributed as a centered Gaussian. Three types of kriging derive from the assumption made on the form of y. In simple kriging, $y(\underline{x}) = \beta_0$ where β_0 is the mean computed from the observations g^{obs}. In ordinary kriging, $y(x) = \beta$ where β is an unknown constant. In universal kriging, $y(\underline{x}) = \underline{f}(\underline{x})^T\underline{\beta}$ where $\underline{f}(\underline{x}) = [f_1(\underline{x}), \ \dots \ , f_k(\underline{x})]$ is a vector containing k basis functions generally chosen as polynomials. To remain general, universal kriging will be considered in this paragraph.

The estimation $\hat{g}$ of g is chosen as a linear combination of observations:

$$\hat{g}(\underline{x}) = \underline{w}(\underline{x})^T\underline{g}^{obs}, \tag{24}$$

where $\underline{w}(\underline{x})$ are the kriging coefficients to be determined.

$\hat{g}$ is searched as the best linear unbiased predictor, which reads:

$$\begin{cases} \mathbb{E}[\hat{g} - G] = 0 \\ \beta = \arg\min \mathbb{E}[(\hat{g} - G)^2], \end{cases} \tag{25}$$

where $\mathbb{E}$ is the expectation.

Solving system (25) using Equations (24) and (23) enables to determine the kriging coefficients. However, it requires the estimation of the covariance matrix of the data $\mathbb{E}(\underline{z}^{obs}\underline{z}^{obs^T})$, where $\underline{z}^{obs} = \underline{g}^{obs} - [y(\underline{x}_1^{obs}), \dots, y(\underline{x}_m^{obs})]$. Generally, the form of the correlation function is chosen a priori. In this article, we use a Gaussian correlation function as it was observed in Reference 39 to give a better approximation than other standard correlation functions for several test cases. Therefore:

$$\mathbb{E}(\underline{z}_{obs}\underline{z}_{obs}^T) = \sigma^2\mathbf{R} = \sigma^2\left[\prod_{k=1}^{n} e^{-\left(\frac{x_k^{obs,i} - x_k^{obs,j}}{\theta_k}\right)^2}\right]_{i,j\in[\![1,m]\!]}, \tag{26}$$

where σ^2 and $\underline{\theta} = [\theta_1, \dots, \theta_n]$ are, respectively, the variance of the process and the vector containing the fluctuation parameters. The fluctuation parameter, or correlation length, can be interpreted as a smoothness parameter: the higher its value, the farther two samples are correlated. These parameters are called hyperparameters.

Several methods exist to estimate σ^2 and θ: the variograms,[40] the leave one-out method,[41] or the maximum likelihood estimation.[42] In this article, the maximum likelihood estimation is considered as it is asymptotically optimal (see p. 124, Reference 43). The likelihood that the data is an outcome of a Gaussian process can be written:

$$\mathcal{L}(\sigma^2, \underline{\theta}) = \frac{1}{\sqrt{(2\pi\sigma^2)^m \ \det \ \mathbf{R}}} e^{-\frac{\underline{z}_{obs}\mathbf{R}^{-1}\underline{z}_{obs}}{2\sigma^2}}, \tag{27}$$

where det$\mathbf{R}$ is the determinant of the correlation matrix. Then $\hat{\theta}$ is determined as

$$\underline{\hat{\theta}} = \text{argmin}_{\underline{\theta}}(-\log(\mathcal{L}(\sigma^2, \underline{\theta}))). \tag{28}$$

Once $\underline{\hat{\theta}}$ is known, the variance σ^2 is computed by calculating stationary points of $\mathcal{L}$, which leads to:

$$\sigma^2 = \frac{\underline{z}_{obs}\mathbf{R}^{-1}\underline{z}_{obs}}{m}. \tag{29}$$

Once the hyperparameters are determined, the optimization system (25) can be solved using the Lagrangian method.

In addition to the estimator $\hat{g}$, kriging metamodeling provides an estimation of the uncertainty on $\hat{g}$ with the variance $s_{\hat{g}}^2$.

3.2 | Adaptive kriging

Using a kriging metamodel allows evaluating the uncertainty on the output through $s_{\hat{g}}^2$. Therefore, the metamodel can be improved by adding observations on points corresponding to large uncertainty on $\hat{g}$. This strategy is developed for reliability analysis in Reference 44 where the learning function chosen for enrichment is:

$$\underline{x} \to U(\underline{x}) = \frac{|\hat{g}(\underline{x})|}{s_{\hat{g}}^2(\underline{x})}. \tag{30}$$

Low U value corresponds to samples close to the limit state ($\hat{g} = 0$) with high uncertainty (high $s_{\hat{g}}^2$ value). Therefore, the limit state function g can be computed at the minimizer of the learning function and added to the observations, which results in the construction of a better metamodel. Then, the metamodel is used to estimate the probability of failure with Monte Carlo estimation:[45]

$$\hat{P}_{f,H} \approx \frac{1}{n_{MC}} \sum_{i=1}^{n_{MC}} ind_{\hat{g}_H \le 0}(X_i), \tag{31}$$

where $ind_{\hat{g}_H \leq 0}$ is the indicator function of the failure domain $\hat{g}_H \leq 0$.

Further details on the algorithm can be found in Reference 44.

3.3 | Multifidelity kriging

We propose a methodology to construct a multifidelity kriging-based metamodel using computations from different meshes corresponding to different levels of fidelity. The refinement strategy is based on guaranteeing the classification of samples used to build the surrogate. For a realization $\underline{x}_i$ of the random variables, the finite element code provides the values $g_H(\underline{x}_i) = R - \tilde{L}(\underline{u}_H)$ and the error estimation enables to obtain $g_m(\underline{x}_i) = R - \tilde{L}(\underline{u}_H) - I_{hh}$ and bounds on $g_{ex}(\underline{x}_i)$ using Equation (17).

If the bounds have the same sign, the state of the point $\underline{x}_i$ (safe or failure) is guaranteed. If not, it means that the discretization error may lead to a wrong classification of the point. Thus, a finer mesh can be defined and used for a new finite element solving for the same random variable realization.

The algorithm we propose is given in Algorithm 1.

Algorithm 1. MF-AK

Choose a coarsest mesh size h_{max} and a finest mesh size h_{min} ;
Generate Monte Carlo (MC) population;
Generate n_1 samples for initialization;
for $i = 1..n_1$ **do**
  Evaluate g_H, g_- and g_+ on $\underline{x}_i$;
  while $g_- g_+ < 0$ *and* $h_{min} \leq h$ **do**
    Perform the remeshing stategy ;
    Evaluate g_H, g_- and g_+ on $\underline{x}_i$;
  end
end
Construct the metamodel $\hat{g}$ and evaluate it on the MC population;
Compute the learning function U;
Compute the failure probability with the metamodel $\hat{g}$;
Compute the coefficient of variation COV of the failure probability;
while $min(U) \leq 2$ *or* $COV > \zeta$ **do**
  while $min(U) \leq 2$ **do**
    Select the learning point $\underline{x}_{new} = \text{argmin}(U)$;
    Evaluate g_H, g_- and g_+ on $\underline{x}_{new}$;
    while $g_- g_+ < 0$ *and* $h_{min} \leq h$ **do**
      Perform the remeshing stategy;
      Evaluate g_H, g_- and g_+ on $\underline{x}_{new}$;
    end
    Construct the metamodel $\hat{g}$ and evaluate it on the MC population;
    Compute the learning function U;
  end
  Compute the failure probability with the metamodel $\hat{g}$;
  Compute the coefficient of variation COV of the failure probability;
  if $COV > \zeta$ **then**
    Enrichment of the Monte Carlo population;
    Evaluate the metamodel on the population;
    Compute the learning function U;
  end
end

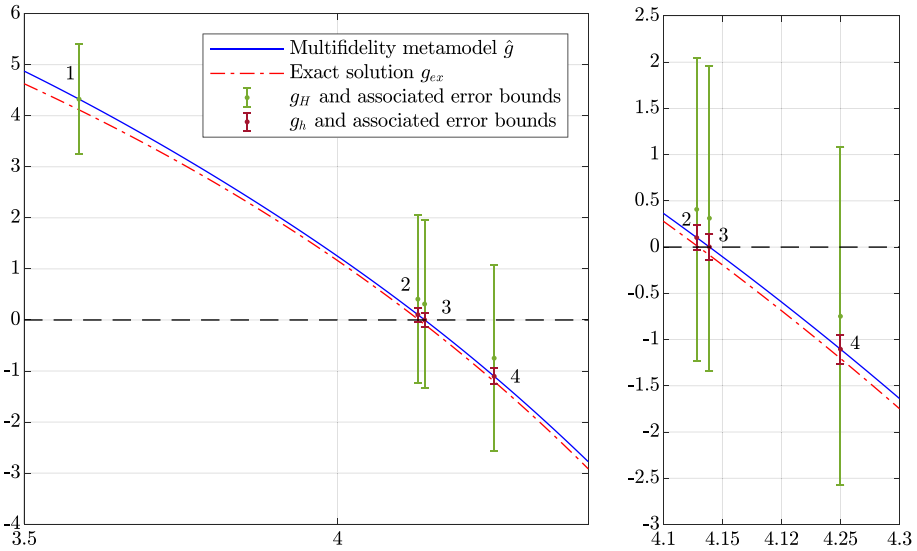

(A) (B) Zoom

FIGURE 1 Exact limit state and multifidelity metamodel built with two level of fidelity g_H and g_h (respectively, mesh size 0.5 and 0.05 m - Number indicates sample index) [Color figure can be viewed at wileyonlinelibrary.com]

This algorithm requires two new parameters compared to classical AK-MCS: the size of the coarsest mesh and the size of the finest mesh. Moreover, a remeshing strategy has to be defined. Several methods can be proposed. The first strategy is to create a family of meshes ranked from coarsest to finest prior to the reliability analysis. A second strategy would be to exploit the error maps provided by the error estimation procedure to generate adaptive mesh. Yet, for quantity of interest, this procedure is not straightforward, as illustrated in Reference 46. If the convergence rate with respect to the mesh size α is known, a third strategy can be defined. From an error estimation on a mesh of size l_c and by doing the hypothesis that reducing the mesh size reduces the interval at a convergence rate $l_c^{2\alpha}$ but does not translate the error interval, then, the optimal mesh size l_{opt} can be computed as

$$l_{c,opt} = l_c \left(\frac{2|g_m|}{e_{CR_\Omega}(\underline{u}_H, \underline{\underline{\hat{\sigma}}}_H) e_{CR_\Omega}(\underline{\tilde{u}}_{\tilde{H}}, \underline{\underline{\hat{\tilde{\sigma}}}}_{\tilde{H}})} \right)^{\frac{1}{2\alpha}}. \tag{32}$$

The metamodel is updated using the learning function defined in Equation (30), as it is done in AK-MCS. Once the metamodel is built, the probability of failure is computed through Monte Carlo sampling.

3.4 | Bounds on the probability of failure

For several mechanical problems, the limit state function is known a priori as monotonic against random variables, which enables to compute bounds on the probability of failure as presented in Reference 47. Let assume that there is only one random variable x and that the limit state function decreases against x (for example, see Figure 1). If the bounds calculated for a given realization x^- guarantee that it is in the failure domain (respectively, in the safe domain for x^+), then any sample with a greater value (respectively lower value) of the realization of the random variable is known to be in the failure domain (respectively, safe). For Figure 1, these two samples would be $x^- = x_1$ and $x^+ = x_4$. Indeed, even on the finest mesh, the state of x_2 and x_3 cannot be guaranteed. Bounds on $P_{f,ex}$ can then be computed using the cumulative probability function F associated with the joint probability density function f of the random variable x:

$$F(x^-) > P_{f,ex} > F(x^+). \tag{33}$$

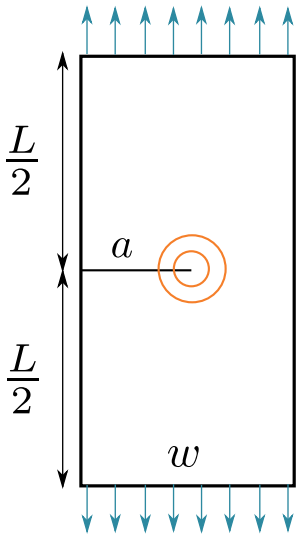

FIGURE 2 Cracked plate with loading of the reference problem (blue) and of the adjoint problem (orange) [Color figure can be viewed at wileyonlinelibrary.com]

4 | NUMERICAL ASSESSMENT

4.1 | Description of the structure

We consider a cracked plate of width $w = 7$m and length $L = 16$m. The length of the crack tip is a, as illustrated on Figure 2. We suppose a linear elastic homogeneous isotropic behavior characterized by the Hooke tensor H. We assume small perturbations, plane strains. Therefore, the mechanical problem is 2D ($d = 2$). $E = 210$ GPa is Young's modulus and $\nu = 0.3$ is the Poisson ratio. The structure undergoes traction with $P = 1$ Pa, which corresponds to mode I opening.

The stress intensity factor K_I is computed using auxiliary solutions and integral over a crown (represented in orange in Figure 2).[48,49] K_I is therefore a linear functional of the displacement $\underline{u}$ and this linear functional defines the loading of the adjoint problem. The Griffith criterion[50] is used as the limit state function $G = K_{lim} - K_I$ where K_{lim} is the critical value. For this structure, empirical expressions of the stress intensity factor K_I are provided in Reference 51. The following is guaranteed with at most 0.5% error:

$$K_{I,ex} = \left(\sqrt{\frac{2w}{\pi a}} \tan \frac{\pi a}{2w} \frac{0.752 + 2.02\frac{a}{w} + 0.37\left(1 - \sin \frac{\pi a}{2w}\right)^3}{\cos \frac{\pi a}{2w}} \right) P\sqrt{\pi a}. \tag{34}$$

This expression will be used to compute the reference exact solution of the problem g_{ex}.

The length a is modeled as a random variable with beta distribution bounded between 1.6 and 4.25 m and of shape parameters both equal to 2.

4.2 | Illustration of the influence of the discretization error on estimation of the probability of failure

Considering K_{lim} deterministic, the exact probability of failure is computed from Equation (34) knowing the cumulative distribution function of a. The lack of precision of formula (34) (0.5%) is propagated on the probability of failure. These two probabilities obtained are referred as mesh size 0^- and 0^+ in Table 2. The middle of these bounds is 0^m. We note $\epsilon = \frac{P_f - P_f(0^m)}{P_f(0^m)}$ the relative error.

The algorithm AK-MCS is used to estimate the failure probability for different mesh sizes l and for two values of K_{lim}: $K_{lim} = 14Pa\sqrt{m}$ and $K_{lim} = 9Pa\sqrt{m}$ for considering two order of magnitude of P_f, namely, 10^{-3} and 10^{-1}. The parameters of AK-MCS are depicted in Table 1. All the metamodels are built using the DACE toolbox.[39] The same Monte Carlo population is used for every simulation.

TABLE 1 AK-MCS parameters

Stopping criterion on learning	**2**
Coefficient of variation criterion ζ	10^{-2}
Size of initial Monte-Carlo population	1000
Type of initialization	Factorial experiment
Initial correlation length	0.55 m
Number of samples to build initial metamodel	5
Maximal factor to multiply $\mathbf{P}_{MC}$ between two iterations	5

TABLE 2 Probabilities of failure and relative error for different mesh sizes and resistance values

	$K_{lim} = 9Pa\sqrt{m}$		$K_{lim} = 14Pa\sqrt{m}$	
l	P_f	ϵ	P_f	ϵ
0^-	$2.23\ 10^{-1}$	0.02	$5.27\ 10^{-3}$	0.12
0^m	$2.27\ 10^{-1}$	0	$5.98\ 10^{-3}$	0
0^+	$2.31\ 10^{-1}$	0.02	$6.72\ 10^{-3}$	0.12
0.5m	$1.40\ 10^{-1}$	0.38	0	1
0.4m	$1.71\ 10^{-1}$	0.25	0	1
0.3m	$1.82\ 10^{-1}$	0.20	$3.79\ 10^{-5}$	0.99
0.2m	$1.94\ 10^{-1}$	0.14	$1.10\ 10^{-4}$	0.90
0.1m	$2.11\ 10^{-1}$	0.07	$2.46\ 10^{-3}$	0.59
0.05m	$2.19\ 10^{-1}$	0.03	$3.91\ 10^{-3}$	0.35
0.02m	$2.24\ 10^{-1}$	0.01	$4.93\ 10^{-3}$	0.17

The results in terms of probability of failure are gathered in Table 2.

First, we observe that the probability of failure depends on the discretization size l. Second, as a too coarse mesh leads to an overestimation of the stiffness of the structure, the probability of failure is underestimated, which may be dramatic in the context of uncertainty qualification through virtual testing. Finally, to obtain less than 40% error on the probability of failure, a mesh size of $l = 0.5$ m would be sufficient for the case $K_{lim} = 9Pa\sqrt{m}$, while a mesh size $l = 0.05$ m would be needed for the case $K_{lim} = 14Pa\sqrt{m}$. This can be explained by two reasons: the discretization error does not depend linearly on the crack length a and, for comparable precisions, the distribution of a has an influence on the obtained value of failure probability. The latter is depicted by the fact that an error of 0.5% with the empirical formula on K_I leads to a relative error of 12% on the failure probability for the case $K_{lim} = 14Pa\sqrt{m}$ and only 2% for the case $K_{lim} = 9Pa\sqrt{m}$. Therefore, as the conception point is unknown, doing an a priori choice of the discretization size is impossible. Moreover, using the same mesh for different safety studies may still lead to errors.

4.3 | Multifidelity kriging

In this subsection, we apply the new Algorithm 1 with the same parameters as for AK-MCS (see Table 1). The size of the coarsest mesh is 0.5 m and the size of the finest mesh is 0.05 m. In the first subsection, we compare different refinement strategies. In the second subsection, we compare our metamodel to a multifidelity metamodel built by evofusion[52] in terms of estimated failure probability and computational time. Each strategy is simulated on five different Monte-Carlo populations in order to assess the robustness of the method.

4.3.1 | Comparison of refinement strategies

Several simulations were done with different sets of intermediate mesh sizes between the coarsest (0.5 m) and the finest (0.05 m). The five different Monte Carlo populations are denoted by P1 to P5 in Table 3. The table reads as follows. Let us

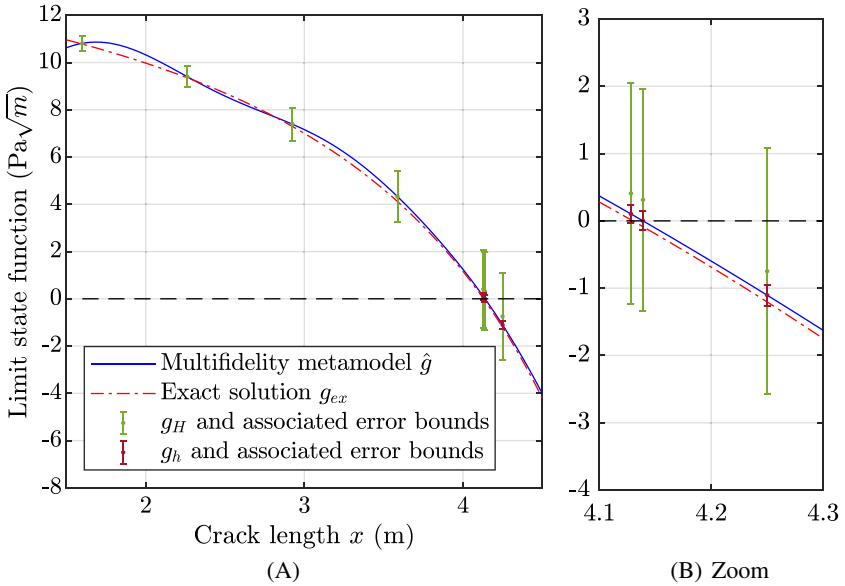

FIGURE 3 Exact limit state and multifidelity metamodel built with two level of fidelity g_H and g_h (respectively, mesh size 0.5 and 0.05 m) [Color figure can be viewed at wileyonlinelibrary.com]

take the example of simulation 6 on population P5. There were 10 calls to the FEM solver on mesh size 0.5 m, among them 4 had two bounds of different sign. The FEM solver was called on mesh size 0.2 m for these 4 samples. Three samples among those 4 had an undetermined state, the FEM was called on the finest mesh (0.05 m) for each of them.

Simulation 1 considers five meshes of size l=[0.5 m, 0.4 m, 0.3 m, 0.2 m, 0.1 m, 0.05 m]. Simulations 2 to 4 correspond to reductions in the number of intermediary meshes between the coarsest and the finest of one level. In a same way, simulations 5 to 7 correspond to a reduction of two in the number of intermediary meshes between the coarsest and the finest. Simulation 8 considers only two possible meshes, the coarsest and the finest. Finally, simulation 9 considers only one possible mesh, which is the finest.

To begin with, whatever the intermediate meshes and the Monte Carlo population, the method converges to the same probability of failure as the one with only the finest mesh, thus proving the robustness of the method. One will note that this probability of failure is different from the one with the same mesh presented in Table 2. The reason is that the metamodel is built with the values g_m. It has been observed that g_m is usually a better approximation than g_H.

Moreover, whatever the intermediate mesh sizes and population, the method is faster than AK-MCS on the finest mesh using g_m (Simulation 9).

From Table 3, we can observe that on average, increasing the number of possible meshes improves the repartition of simulations between the different levels of fidelity. However, it also increases the average CPU time as some evaluations may not be useful to determine the sign of the limit state function. This is highlighted by simulation 5 on population 1 (S5P1) where only necessary levels of fidelity according to S1P1 are considered. The difference in CPU time is also attributable to a greater number of samples being evaluated during enrichment. It is to be noticed that S2P1 is shorter than simulation S3P1 and S4P1. The reason is a smaller number of calls to the finest mesh.

Figure 3 shows the limit state function against the crack length. It shows that samples close to the limit state are calculated on the finest mesh, which is paramount when building a multifidelity metamodel for reliability purposes. It is to be noted that every sample added during enrichment phase is calculated on the finest mesh.

As highlighted, it is not trivial to choose more than two levels of fidelity as the best repartition depends on the quality of bounds, the limit state function and samples for which the finite element solver will be called. It is therefore suggested to only use the coarsest and finest mesh.

This strategy is compared with the one exploiting the computation of an optimal mesh size l_{opt}. The results are presented in Table 4. This table is presented in a different way than Table 3. Each column corresponds to one sample added to the metamodel and each row within each column corresponds to the intermediate mesh sizes used for this sample. For example, for the strategy with optimal mesh size on population 1, the four first samples used to initialize the metamodel are guaranteed by the bounds on the coarsest mesh. However, the fifth sample is not guaranteed and is therefore calculated on a finer mesh (ie, 0.21 m) and its state is then guaranteed. During the enrichment phase, two samples were added to the metamodel and were both calculated on mesh size 0.059 and 0.05 m (finest mesh). The second part of Table 4 presents simulation 8 from Table 3 and serves as a reference for comparaison with the optimal mesh size estimation strategy.

TABLE 3 Comparison of refinements strategies: P stands for population and S stands for simulation

	Mesh size																													
	0.5m					0.3m					0.2m					0.1m					0.05m					$P_f \times 10^{-3}$	CPU time $\times 10^3$s				
S	P1	P2	P3	P4	P5	P1	P2	P3	P4	P5	P1	P2	P3	P4	P5	P1	P2	P3	P4	P5	P1	P2	P3	P4	P5		P1	P2	P3	P4	P5
1	10	7	7	7	10	4	3	3	3	4	3	3	3	3	4	3	2	2	2	3	3	2	2	2	3	5.1 for all	8	6	6	6	9
2	7	7	7	7	10						3	3	3	3	4	2	2	2	2	3	2	2	2	2	3	5.1 for all	6	5	6	6	8
3	10	6	6	6	6	4	2	2	2	2						3	2	2	2	2	3	1	1	1	1	5.1 for all	8	3	6	3	3
4	10	7	7	7	10	4	3	3	3	4	3	3	3	3	4						3	2	2	2	3	5.1 for all	7	5	5	5	7
5	10	7	7	7	7	4	3	3	3	3											3	3	3	3	3	5.1 for all	7	6	6	4	6
6	7	7	7	7	10						3	3	3	3	4						2	2	2	2	3	5.1 for all	5	5	5	5	7
7	6	6	7	6	6											2	2	3	2	2	1	1	2	1	1	5.1 for all	3	3	5	3	3
8	7	7	7	6	7																3	3	3	2	3	5.1 for all	6	6	6	4	6
9																					7 for all					5.1 for all	13 for all				

TABLE 4 Comparison of strategy between two levels of fidelity (same as Set 8 in Table 3) and optimal mesh size estimation

	Pop.	Mesh size (m)					P_f ($\times 10^{-3}$)	CPU time ($\times 10^3 s$)
With optimal mesh size	1	0.5 (7)	0.21 (1)	0.095 (1)	0.059 (1)	0.05 (1)	5.1	4.1
	2	0.5 (7)	0.21 (1)	0.094 (1)	0.062 (1)	0.05 (1)	5.1	4.3
	3	0.5 (7)	0.21 (1)	0.094 (1)	0.062 (1)	0.05 (1)	5.1	4.2
	4	0.5 (7)	0.21 (1)	0.15 (1)	0.069 (1)	0.05 (2)	5.1	5.9
	5	0.5 (7)	0.21 (1)	0.098 (1)	0.055 (1)	0.05 (1)	5.1	4.0
Without optimal mesh size	1	0.5 (7)	0.05 (3)				5.1	5.8
	2	0.5 (7)	0.05 (3)				5.1	5.6
	3	0.5 (7)	0.05 (3)				5.1	5.6
	4	0.5 (7)	0.05 (2)				5.1	3.8
	5	0.5 (7)	0.05 (3)				5.1	5.7

First, it is to be noted that whatever the Monte Carlo population, the optimal mesh size estimation strategy converges to the same probability of failure as the reference simulation. For most samples, the first optimal mesh size estimation allows to guarantee its state and the strategy finds a coarser mesh than the finest one. The finest mesh is always reached allowing to estimate the same probability of failure as the reference simulation. The finding of a good mesh compromise allows to reduce CPU time on all populations.

In most engineering problems, the mesh size convergence rate is not known a priori. It is therefore not possible to use the optimal mesh size estimation strategy to compute the probability of failure. In this case, it is recommended to only choose a coarse mesh and the fine one.

4.3.2 | Comparison with a metamodel built by evofusion

In Reference 52, the authors propose an approach named evofusion to construct a metamodel from data for multiple levels of fidelity (at least two). Let g_2 and g_1 denote the functions estimated respectively from a high and low fidelity model. g_2 may be written as:

$$g_2 = g_1 + \underbrace{g_2 - g_1}_{g_{err}}. \tag{35}$$

The principle consists in creating a first kriging metamodel for g_1 and a second for g_{err} . The sum of the two metamodels is an evofused metamodel that is built from 2 levels of fidelity. The advantage of using such a metamodel is that the global trend may be captured thanks to low fidelity data. The error metamodel between level 1 and 2 may then be built, thanks to a few calls to both g_1 and g_2. A measure of the uncertainty on the evofused metamodel is computed from the standard deviations of the low-fidelity metamodel and the error metamodel by considering that g_{err} and g_1 are uncorrelated, which gives:

$$s^2_{\hat{g}_2} = s^2_{\hat{g}_1} + s^2_{\hat{g}_{err}}. \tag{36}$$

For readers familiar with co-kriging,[53] Equation (35) is very similar to the co-kriging formulation:

$$g_2 = \rho_1 \times g_1 + \delta_1, \tag{37}$$

where ρ_1 and δ_1 are unknowns.

In fact, evofusion might be seen as the particular case of co-kriging where $\rho_1 = 1$ and $\delta_1 = g_{err}$.

TABLE 5 Evofusion parameters

Stopping criterion on learning	**2**
Coefficient of variation criterion ζ	10^{-2}
Size of initial Monte-Carlo population	1000
Type of initialization	Factorial experiment
Initial correlation length for g_1 and for g_{er}	0.55m
Number of sample to build initial metamodel	5
Maximal factor to multiply $\mathbf{P}_{MC}$ between two iterations	5

TABLE 6 Comparison between evofusion and multifidelity kriging

		Mesh size (m)			
	Pop.	**0.5**	**0.05**	P_f	**CPU time**
Kriging	1	7	3	5.1 for all	6
	2	7	3		6
	3	7	3		6
	4	6	2		4
	5	7	3		6
Evofusion	1	28	5	5.1	6
	2	128	5	5.1	11
	3	Error metamodel not converged			
	4	Low fidelity metamodel not converged			
	5	97	6	5.1	13

In this article, we consider an adaptation of evofusion to AK-MCS. For this purpose, a learning function needs to be introduced. The U function is adapted:

$$x \to U(x) = \frac{|\hat{g}_1(x) + \hat{g}_{err}(x)|}{s^2_{\hat{g}_1}(x) + s^2_{\hat{g}_{err}}(x)}. \tag{38}$$

Given x_i with $U(x_i) < 2$, a refinement strategy is to use the decomposition of $s^2_{\hat{g}}$ as a sum for every level of fidelity. $g_1(x_i)$ could be simulated and added to $\hat{g}_1$, thus reducing $s^2_{\hat{g}}(x_i)$ (as $s^2_{\hat{g}_1}(x_i) = 0$). If $s^2_{\hat{g}}(x_i)$ is still smaller than 2 then a call to the high-fidelity model is necessary.

The low-fidelity model is built from the finite element solution for a mesh size of 0.5 m (no error estimation is performed) and the high-fidelity model is built from g^m (obtained after error estimation) on a mesh size of 0.05 m : the same high fidelity is chosen as the finest mesh from Section 4.3.1 to be able to compare results.

To build an initial metamodel, five samples are selected with a factorial experiment over the whole space on which x^i is defined. g_1 is called for each of them. Three samples are selected among them to calculate g_2 and be able to compute g_{err}. These samples are selected by picking the three values closest to the limit state $g_1 = 0$.

Parameters of the evofusion metamodel are shown in Table 5.

Results

The obtained probabilities of failure and CPU time for both evofusion and multifidelity kriging are given in Table 6.

As shown in Table 6, evofusion does not reduce the number of evaluations needed to estimate the probability of failure. In fact, in simulations for which the method converges, the number of FEM evaluations is still higher than the reference simulation of multifidelity kriging.

For some Monte-Carlo populations, the method using evofusion does not converge. The metamodel and the samples used to build it were inspected. When too many samples are added to the metamodel, it becomes likely that two of them

TABLE 7 Bounds on the probability of failure depending on the refinement strategy and Monte Carlo population (P1 to P5)

	P_f^- ($\times 10^{-3}$)					P_f^+ ($\times 10^{-2}$)				
Set	P1	P2	P3	P4	P5	P1	P2	P3	P4	P5
1	3.8	0	0	0	0	5.7	16	16	16	16
2	3.8	0	0	0	4.0	5.7	16	16	16	16
3	3.8	0	0	0	0	16	16	16	16	16
4	4.1	0	0	0	0	16	16	16	16	16
5	0	0	0	0	0	16	16	16	16	16
6	4.1	0	0	0	4.0	5.7	16	16	16	16
7	3.8	0	0	0	0	5.7	16	16	16	16
8	3.8	0	0	0	0	5.7	16	16	16	16

have very close input values. In order to fit those two samples, the metamodel needs to bend sharply thus making the correlation length drop. Finally, the metamodel uncertainty increases and the number of samples needed to improve its quality plumets: the method never converges. It is possible that the trigger of this problem is the learning function U. In fact, it was seen to call for too many enrichment in Reference 54.

4.3.3 | Bounds on the probability of failure

Bounds on P_f can be computed using samples that are guaranteed to be in the failure domain as highlighted in Section 3.4. Table 7 shows bounds added to simulations from Table 3. Bounds can be thin, in the same range as the one provided in Table 2 with the empirical formula. However, for some cases, there is no guaranteed sample close to the limit state. Nothing guarantees a priori that bounds of good quality will be computed with this method. The best practice would be to add with expertise a few samples close enough to the limit state and with guaranteed sign. In any case, this post-process is extremely cheap and offer an estimation of safety margins.

5 | CONCLUSION

In this article, we presented the construction of a multifidelity kriging-based metamodel for the estimation of the probability of failure. By exploiting discretization error estimators, it is possible to ensure the state (safe or failure) of the points used to build the metamodel. Therefore, the correct classification of those points is guaranteed. It allows to define a strategy to build the metamodel from computations on different mesh sizes thus adapting the discretization to the objective. Such a strategy allows to reduce total computational cost compared to a strategy using a unique mesh size and to focus expensive computations on critical points. Results using a kriging metamodel were compared to the ones using evofusion, a more evolved multifidelity kriging-based metamodel. The initial metamodel appears to be more effective than evofusion as it allows to calculate the same probability of failure with smaller CPU time. When the convergence rate is known, the estimation of an optimal mesh size for classification is proposed. Results obtained were quite similar, thus highlighting the very good performance of the initial strategy.

Future work will consist in extending this approach to more complex reliability problems. Indeed, an increased number of random variables, three-dimensional problems with nonlinear mechanics or a nonlinear quantity of interest will be considered.

ACKNOWLEDGEMENTS

The author would like to thank Florent Pled for the helpful and fruitful discussions. This work was carried out within the project MUSCAS (MUlti-SCAle Stochastic computation for MRE) granted by WEAMEC, West atlantic Marine Energy Community with the support of Région Pays de la Loire and in partnership with Chantiers de l'Atlantique.

CONFLICT OF INTEREST

The authors declare that there is no conflict of interest.

ORCID

V. Rey https://orcid.org/0000-0003-1019-1819
F. Schoefs https://orcid.org/0000-0002-7559-6182

REFERENCES

1. Caflisch RE. Monte Carlo and quasi-Monte Carlo methods. *Acta Numerica*. 1998;7:1-49. https://doi.org/10.1017/S0962492900002804.
2. Giles MB. Multilevel Monte Carlo path simulation. *Oper Res*. 2008;56(3):607-617. https://doi.org/10.1287/opre.1070.0496.
3. Giles MB. Multilevel monte carlo methods. *Acta Numerica*. 2015;24:259.
4. Matthies HG, Keese A. Galerkin methods for linear and nonlinear elliptic stochastic partial differential equations. *Comput Methods Appl Mech Eng*. 2005;194(12-16):1295-1331. https://doi.org/10.1016/j.cma.2004.05.027, http://linkinghub.elsevier.com/retrieve/pii/S0045782504003950.
5. Nouy A, Clement A, Schoefs F, Moës N. An extended stochastic finite element method for solving stochastic partial differential equations on random domains. *Comput Methods Appl Mech Eng*. 2008;197(51-52):4663-4682.
6. Pasqualini O, Schoefs F, Chevreuil M, Cazuguel M. Measurements and statistical analysis of fillet weld geometrical parameters for probabilistic modelling of the fatigue capacity. *Mar Struct*. 2013;34:226-248.
7. Schoefs F. Sensitivity approach for modelling the environmental loading of marine structures through a matrix response surface. *Reliab Eng Syst Saf*. 2008;93(7):1004-1017.
8. Krige D. A statistical approach to some mine valuation and allied problems on the witwatersrand. *J South Afr Inst Min Metall*. 1951;52(6):119-139.
9. Sacks J, Welch WJ, Mitchell TJ, Wynn HP. Design and analysis of computer experiments. *Stat Sci*. 1989;11(4):409-423. https://doi.org/10.1214/ss/1177012413.
10. Echard B, Gayton N, Lemaire M. Ak-mcs: an active learning reliability method combining kriging and Monte Carlo simulation. *Struct Saf*. 2011;33(2):145-154.
11. Echard B, Gayton N, Lemaire M, Relun N. A combined importance sampling and kriging reliability method for small failure probabilities with time-demanding numerical models. *Reliab Eng Syst Saf*. 2013;111:232-240. https://doi.org/10.1016/j.ress.2012.10.008, http://www.sciencedirect.com/science/article/pii/S0951832012002086.
12. Tong C, Sun Z, Zhao Q, Wang Q, Wang S. A hybrid algorithm for reliability analysis combining kriging and subset simulation importance sampling. *J Mech Sci Technol*. 2015;29(8):3183-3193.
13. Fauriat W, Gayton N. Ak-sys: an adaptation of the AK-MCS method for system reliability. *Reliab Eng Syst Saf*. 2014;123:137-144.
14. Zhang J, Xiao M, Gao L, Fu J. A novel projection outline based active learning method and its combination with kriging metamodel for hybrid reliability analysis with random and interval variables. *Comput Methods Appl Mech Eng*. 2018;341:32-52. https://doi.org/10.1016/j.cma.2018.06.032, http://www.sciencedirect.com/science/article/pii/S0045782518303293.
15. Zhang J, Xiao M, Gao L, Chu S. A combined projection-outline-based active learning kriging and adaptive importance sampling method for hybrid reliability analysis with small failure probabilities. *Comput Methods Appl Mech Eng*. 2019;344:13-33. https://doi.org/10.1016/j.cma.2018.10.003, http://www.sciencedirect.com/science/article/pii/S0045782518304997.
16. Rashki M, Ghavidel A, Arab HG, Mousavi SR. Low-Cost Finite Element Method-Based Reliability Analysis Using Adjusted Control Variate Technique. *Struct Saf*. 2018;75:133-142.
17. Alvin KF. Method for treating discretization error in nondeterministic analysis. *AIAA J*. 2000;38(5):910-916.
18. Mahadevan S, Rebba R. Inclusion of model errors in reliability-based optimization. *J Mech Des*. 2006;128(4):936-944.
19. Hasofer AM, Lind NC. Exact and invariant second-moment code format. *J Eng Mech Div*. 1974;100(1):111-121.
20. Gallimard L. Error bounds for the reliability index in finite element reliability analysis. *Int J Numer Methods Eng*. 2011;87(8):781-794.
21. Dadone A, Grossman B. Progressive optimization of inverse fluid dynamic design problems. *Comput Fluids*. 2000;29(1):1-32. https://doi.org/10.1016/S0045-7930(99)00002-X, http://www.sciencedirect.com/science/article/pii/S004579309900002X.
22. de Baar J, Roberts S, Dwight R, Mallol B. Uncertainty quantification for a sailing yacht hull, using multi-fidelity kriging. *Comput Fluids*. 2015;123:185-201.
23. Perdikaris P, Venturi D, Royset J, Karniadakis G. Multi-fidelity modelling via recursive co-kriging and Gaussian–Markov random fields. *Proc R Soc A*. 2015;471(2179):20150 018.
24. Courrier N, Boucard PA, Soulier B. The use of partially converged simulations in building surrogate models. *Adv Eng Softw*. 2014;67:186-197.
25. Courrier N, Boucard PA, Soulier B. Variable-fidelity modeling of structural analysis of assemblies. *J Glob Optim*. 2016;64(3):577-613.
26. Nachar S, Boucard PA, Néron D, Bordeu F. Coupling multi-fidelity kriging and model-order reduction for the construction of virtual charts. *Comput Mech*. 2019;64(6):1685-1697. https://doi.org/10.1007/s00466-019-01745-9, https://hal.archives-ouvertes.fr/hal-02169052.
27. Ainsworth M, Oden JT. A posteriori error estimation in finite element analysis. *Comput Methods Appl Mech Eng*. 1997;142(1-2):1-88.
28. Ladevèze P, Pelle JP. *Mastering Calculations in Linear and Nonlinear Mechanics*. New York, NY: Springer; 2004.
29. Ladevèze P, Leguillon D. Error estimate procedure in the finite element method and application. *SIAM J Numer Anal*. 1983;20(3):485-509.

30. Parés N, Díez P, Huerta A. Subdomain-based flux-free a posteriori error estimators. *Comput Methods Appl Mech Eng*. 2006;195(4-6):297-323. https://doi.org/10.1016/j.cma.2004.06.047.
31. Pled F, Chamoin L, Ladevèze P. On the techniques for constructing admissible stress fields in model verification: performances on engineering examples. *Int J Numer Methods Eng*. 2011;88(5):409-441. https://doi.org/10.1002/nme.3180.
32. Rey V, Gosselet P, Rey C. Study of the strong prolongation equation for the construction of statically admissible stress fields: implementation and optimization. *Comput Methods Appl Mech Eng*. 2014;268(0):82-104. https://doi.org/10.1016/j.cma.2013.08.021.
33. Becker R, Rannacher R. A feed-back approach to error control in finite element methods: basic analysis and examples. *J Numer Math*. 1996;4:237-264.
34. Strouboulis T, Babuška I, Datta D, Copps K, Gangaraj S. A posteriori estimation and adaptive control of the error in the quantity of interest. Part I: posteriori estimation of the error in the von mises stress and the stress intensity factor. *Comput Methods Appl Mech Eng*. 2000;181(1-3):261-294.
35. Rüter M, Stein E. Goal-oriented a posteriori error estimates in linear elastic fracture mechanics. *Comput Methods Appl Mech Eng*. 2006;195(4-6):251-278.
36. Ladevèze P. Upper error bounds on calculated outputs of interest for linear and nonlinear structural problems. *Comptes Rendus Académie des Sciences - Mécanique, Paris*. 2006;334(7):399-407. https://doi.org/10.1016/j.crme.2006.04.004.
37. Ladevèze P. Strict upper error bounds on computed outputs of interest in computational structural mechanics. *Comput Mech*. 2008;42(2):271-286. https://doi.org/10.1007/s00466-007-0201-y.
38. Mallik G, Vohralík M, Yousef S. Goal-oriented a posteriori error estimation for conforming and nonconforming approximations with inexact solvers. *J Comput Appl Math*. 2020;366:112-367.
39. Lophaven SN, Nielsen HB, Søndergaard J. *Aspects of the matlab toolbox DACE. The Technical University of Denmark: IMM, Informatics and Mathematical Modelling*. 2002.
40. Matheron G. *Les variables régionalisées et leur estimation: une application de la théorie des fonctions aléatoires aux sciences de la nature*. Université de Virginie: Masson et CIE; 1965.
41. Rippa S. An algorithm for selecting a good value for the parameter c in radial basis function interpolation. *Adv Comput Math*. 1999;11(2-3):193-210.
42. Sacks J, Welch WJ, Mitchell TJ, Wynn HP. Design and analysis of computer experiments. *Stat Sci*. 1989;4:409-423.
43. Wasserman L. *All of Statistics: A Concise Course in Statistical Inference*. Springer Science & Business Media; 2013.
44. Echard B. Assessment by Kriging of the Reliability of Structures Subjected to Fatigue Stress (PhD thesis); 2012.
45. Metropolis N, Ulam S. The Monte Carlo method. *J Am Stat Assoc*. 1949;44(247):335-341.
46. Diez P, Calderon G. Remeshing criteria and proper error representations for goal oriented h-adaptivity. *Comput Methods Appl Mech Eng*. 2007;196(4-6):719-733.
47. de Rocquigny E. Structural reliability under monotony: properties of form, simulation or response surface methods and a new class of monotonous reliability methods (mrm). *Struct Saf*. 2009;31(5):363-374. https://doi.org/10.1016/j.strusafe.2009.02.002, http://www.sciencedirect.com/science/article/pii/S0167473009000162.
48. Stern M, Becker EB, Dunham RS. A contour integral computation of mixed-mode stress intensity factors. *Int J Fract*. 1976;12(3):359-368.
49. Gallimard L, Panetier J. Error estimation of stress intensity factors for mixed-mode cracks. *Int J Numer Methods Eng*. 2006;68(3):299-316. https://doi.org/10.1002/nme.1705.
50. Griffith A. The phenomena of rupture and flow in solids. *Philos Trans R Soc Lond*. 1921;221:163-198.
51. Tada H, Paris PC, Irwin GR. The stress analysis of cracks Handbook. Hellertown: Del Research Corporation; 1973.
52. Forrester AI, Bressloff NW, Keane AJ. Optimization using surrogate models and partially converged computational fluid dynamics simulations. *Proc Royal Soc A Math Phys Eng Sci*. 2006;462(2071):2177-2204.
53. Kennedy MC, O'Hagan A. Predicting the output from a complex computer code when fast approximations are available. *Biometrika*. 2000;87(1):1-13.
54. Gaspar B, Teixeira A, Soares CG. A study on a stopping criterion for active refinement algorithms in kriging surrogate models. *Safety Reliab Compl Eng Syst*. 2015;1219-1227.

SUPPORTING INFORMATION

Additional supporting information may be found online in the Supporting Information section at the end of this article.

How to cite this article: Mell L, Rey V, Schoefs F. Multifidelity adaptive kriging metamodel based on discretization error bounds. *Int J Numer Methods Eng*. 2020;1–18. https://doi.org/10.1002/nme.6451